

Simulation of the traveling wave burning on epithermal neutrons on the year time scale

V.D. Rusov^{a,*}, V.A. Tarasov^a, M.V. Eingorn^b, S.A. Chernezhenko^a, A.A. Kakaev^a,
V.P. Smolyar^a, S.I. Kosenko^a, T.N. Zelentsova^a

^a*Department of Theoretical and Experimental Nuclear Physics, Odessa National Polytechnic University,
Shevchenko av. 1, Odessa 65044, Ukraine*

^b*CREST and NASA Research Centers, North Carolina Central University, Fayetteville st. 1801, Durham,
North Carolina 27707, U.S.A.*

Abstract

We present the newly obtained results of two computer simulations of the epithermal neutron-nuclear burning in natural uranium. Each of them modeled the period of six months of the traveling wave reactor (TWR) operation – for two different flux densities of an external neutron source.

The simulation results confirm the existence of a nuclear burning wave at longer time scales, and reveal the dependence of the wave burning modes on the parameters of an external neutron source.

1. Introduction

Following our previous work on numerical modeling of a wave burning in natural uranium on epithermal neutrons [1], here we present another two simulation results which confirm the possibility of the wave nuclear burning in natural uranium in the epithermal region of neutron energies.

The first simulation reproduces the last example simulation in [1], but for a much longer period of time. In this case the neutron flux density was $10^{23} \text{ neutron/cm}^2 \cdot \text{s}$ and the simulated reactor operation time was 150 days (as against 48 days in [1]).

Another calculation was carried out for an external source with a significantly lower flux density equal to $10^{15} \text{ neutron/cm}^2 \cdot \text{s}$ and for a simulation time of 150 days.

2. New simulation results of a wave neutron-nuclear burning in natural uranium on epithermal neutrons

Figures 1-5 show the simulation results for the neutron flux density of an external source equal to $10^{23} \text{ cm}^{-2} \cdot \text{s}^{-1}$. The kinetic system of 20 equations, the initial and boundary conditions remained the same as in [1]. The only difference here is the simulated operation time.

In the present work, as in [1], the numerical solution of the system of kinetic equations was carried out using the Mathematica 8 software package. In order to optimize the process of numerical solution of the system of equations, we switched to dimensionless variables $n(x, t) \rightarrow n^*(x, t)$ and $N(x, t) \rightarrow N^*(x, t)$, according to the following relations:

$$n(x, t) = \frac{\Phi_0}{V_n} n^*(x, t), \quad N(x, t) = \frac{\rho_8 N_A}{\mu_8} N^*(x, t). \quad (1)$$

In the first calculation, the following constants were used:

*Corresponding author e-mail: siiiis@te.net.ua

$$D = 2.0 \cdot 10^4 \text{ cm}^2/\text{s}; \quad V_n = 1.0 \cdot 10^6 \text{ cm}/\text{s}; \quad \Phi_0 = 1.0 \cdot 10^{23} \text{ cm}^{-2}\text{s}^{-1}; \quad \tau_\beta \sim 3.3 \text{ days};$$

$$\nu^{(Pu)} = 2.90; \nu^{(5)} = 2.41;$$

$$\sigma_f^{Pu} = 477.04 \cdot 10^{-24} \text{ cm}^2; \quad \sigma_c^{Pu} = 286.15 \cdot 10^{-24} \text{ cm}^2; \quad \sigma_c^8 = 252.50 \cdot 10^{-24} \text{ cm}^2;$$

$$\sigma_f^5 = 136.43 \cdot 10^{-24} \text{ cm}^2; \quad \sigma_c^5 = 57.61 \cdot 10^{-24} \text{ cm}^2; \quad \sigma_c^9 = 4.80 \cdot 10^{-24} \text{ cm}^2;$$

$$\sigma_c^{eff(Pu)} = 10.10 \cdot 10^{-24} \text{ cm}^2; \quad \sigma_c^{i(Pu)} = 1.00 \cdot 10^{-24} \text{ cm}^2, i = 1..6;$$

$$\sigma_c^{eff(5)} = 10.10 \cdot 10^{-24} \text{ cm}^2; \quad \sigma_c^{i(5)} = 1.00 \cdot 10^{-24} \text{ cm}^2, i = 1..6;$$

$$T_1^{(Pu)} = 54.28 \text{ s}; \quad T_2^{(Pu)} = 23.04 \text{ s}; \quad T_3^{(Pu)} = 5.60 \text{ s};$$

$$T_4^{(Pu)} = 2.13 \text{ s}; \quad T_5^{(Pu)} = 0.62 \text{ s}; \quad T_6^{(Pu)} = 0.26 \text{ s};$$

$$p_1^{(Pu)} = 0.072 \cdot 10^{-3}; \quad p_2^{(Pu)} = 0.626 \cdot 10^{-3}; \quad p_3^{(Pu)} = 0.444 \cdot 10^{-3};$$

$$p_4^{(Pu)} = 0.685 \cdot 10^{-3}; \quad p_5^{(Pu)} = 0.180 \cdot 10^{-3}; \quad p_6^{(Pu)} = 0.093 \cdot 10^{-3};$$

$$p^{(Pu)} = \sum_{i=1}^6 p_i^{(Pu)} = 0.0021; \quad \sigma_c^{eff} = 1.10 \cdot 10^{-24} \text{ cm}^2;$$

$$T_1^{(5)} = 55.72 \text{ s}; \quad T_2^{(5)} = 22.72 \text{ s}; \quad T_3^{(5)} = 6.22 \text{ s};$$

$$T_4^{(5)} = 2.30 \text{ s}; \quad T_5^{(5)} = 0.61 \text{ s}; \quad T_6^{(5)} = 0.23 \text{ s};$$

$$p_1^{(5)} = 0.210 \cdot 10^{-3}; \quad p_2^{(5)} = 1.400 \cdot 10^{-3}; \quad p_3^{(5)} = 1.260 \cdot 10^{-3};$$

$$p_4^{(5)} = 2.520 \cdot 10^{-3}; \quad p_5^{(5)} = 0.740 \cdot 10^{-3}; \quad p_6^{(5)} = 0.27 \cdot 10^{-3};$$

$$p^{(5)} = \sum_{i=1}^6 p_i^{(5)} = 0.0064. \tag{2}$$

The length of the fissile medium, in which the wave of neutron-nuclear burning propagates, is 1000 cm, the total simulation time is $t = 150 \text{ days}$, the time step is $\Delta t = 10 \text{ minutes}$, and the spatial step is $\Delta x = 1 \text{ cm}$.

As can be seen from the presented results, e.g. in Fig. 5, after 90 days the amplitude of the ^{239}Pu concentration reaches a stationary maximum. This maximum of plutonium has shifted by 20 cm over 60 days, which allows us to estimate the speed of steady-state wave burning, which is approximately equal to $0.39 \cdot 10^{-5} \text{ cm}/\text{s}$. It was not possible to make such an estimation in [1] because of the short simulation time of 48 days.

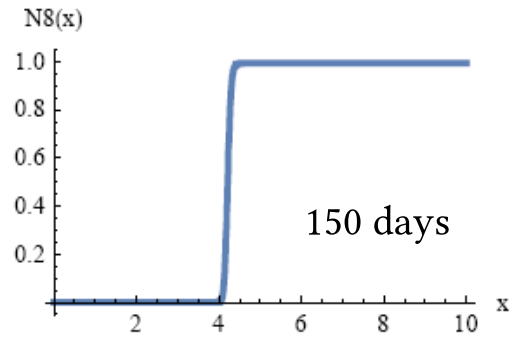
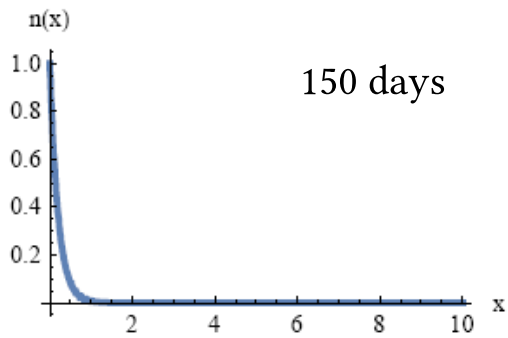
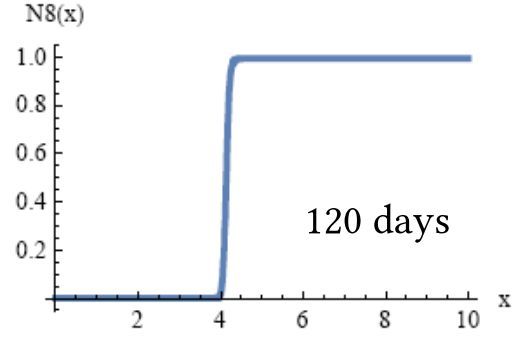
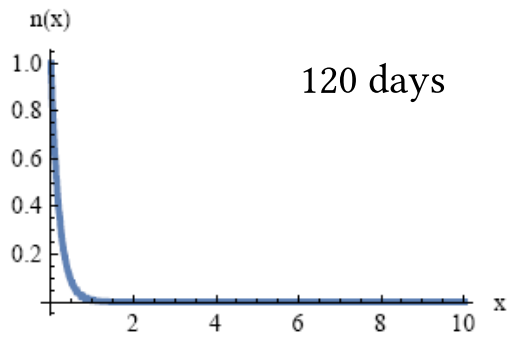
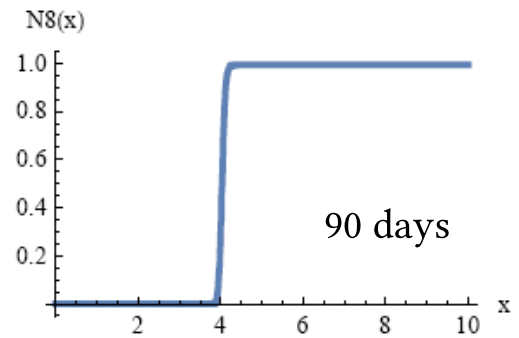
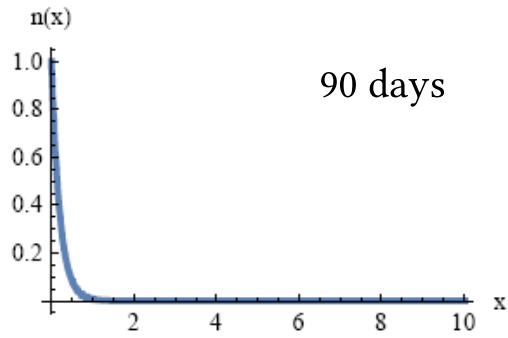
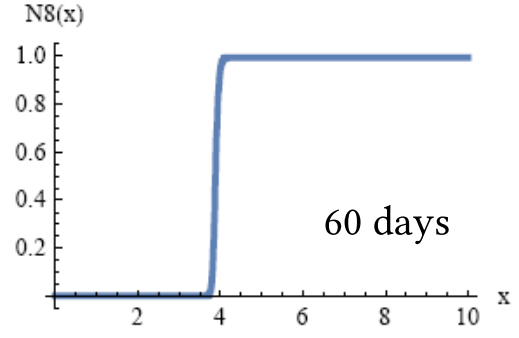
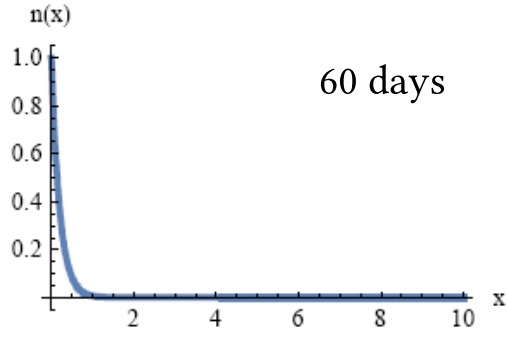
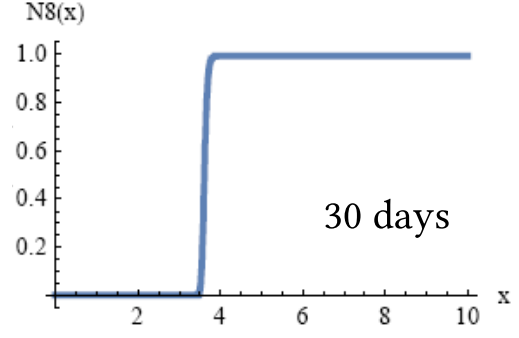
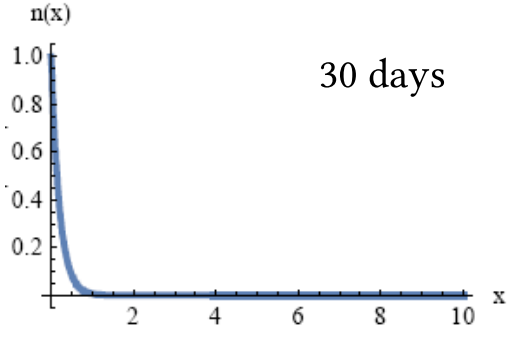


Figure 1: Kinetics of the neutrons density during the wave nuclear burning in natural uranium. The dimensionless neutron density is plotted.

Figure 2: Kinetics of the ^{238}U density during the wave nuclear burning in natural uranium. The dimensionless ^{238}U density is plotted.

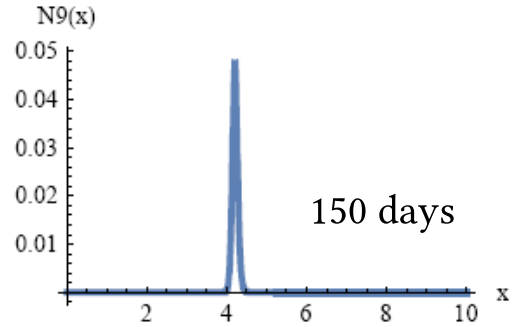
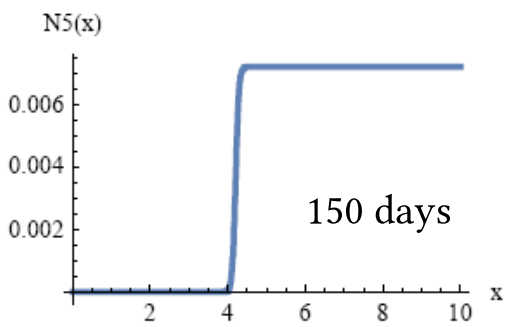
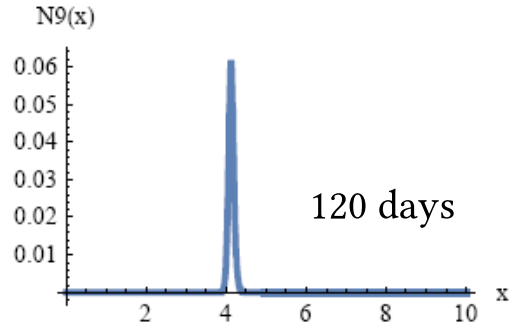
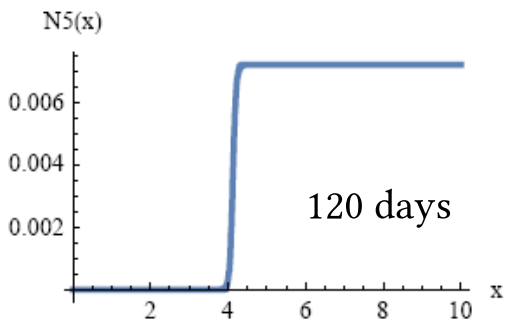
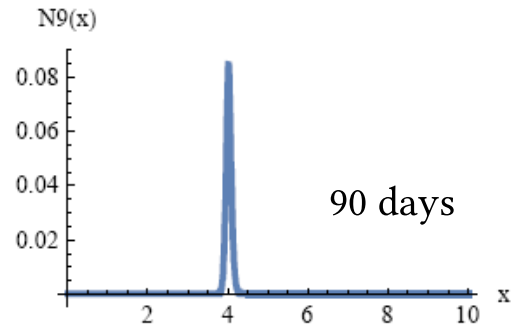
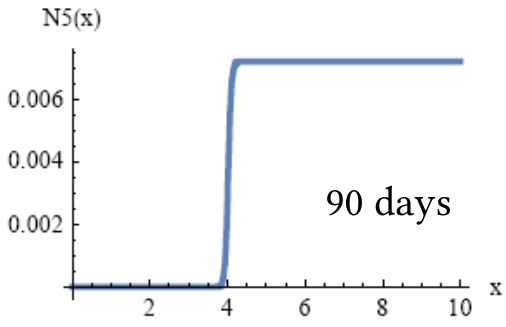
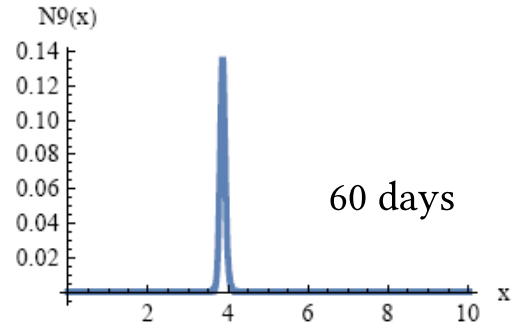
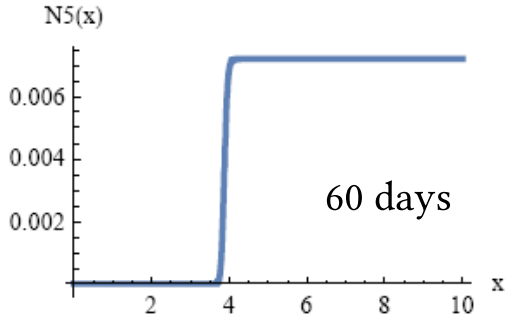
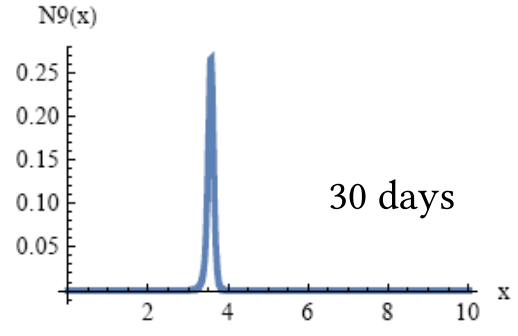
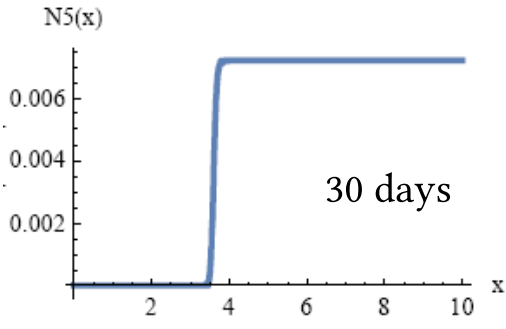


Figure 3: Kinetics of the ^{235}U density during the wave nuclear burning in natural uranium. The dimensionless ^{235}U density is plotted.

Figure 4: Kinetics of the ^{239}U density during the wave nuclear burning in natural uranium. The dimensionless ^{239}U density is plotted.

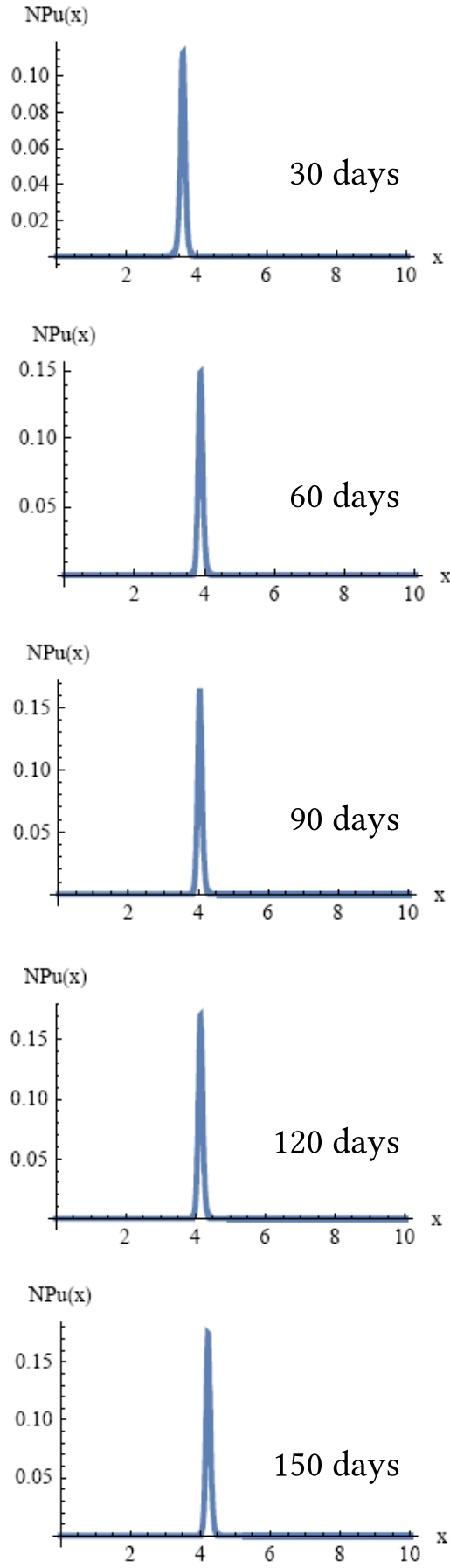


Figure 5: Kinetics of the ^{239}Pu density during the wave nuclear burning in natural uranium. The dimensionless ^{239}Pu density is plotted.

Below in Figures 6-10 we show the simulation results for the same kinetic system, the same basic calculation constants (see (2)), and the same initial and boundary conditions, except for the value for the external neutron flux density, equal in this case to $10^{15} \text{ cm}^{-2}\text{s}^{-1}$. The length of the fissile medium in which the wave of neutron-nuclear burning propagates is 1000 cm, the total simulation time is $t = 150 \text{ days}$, the temporal step is $\Delta t = 5 \text{ minutes}$, and the spatial step is $\Delta x = 1 \text{ cm}$.

From the presented results, e.g. Fig. 10, it can be seen that after 60 days the amplitude of the ^{239}Pu concentration reaches a steady maximum, which shifts by 60 cm during the simulated period of 90 days. This allows us to estimate the speed of steady-state wave burning, which is approximately equal to

$$u_{calc} \approx 60 \text{ cm} / (90 \cdot 24 \cdot 3600 \text{ s}) \approx 0.77 \cdot 10^{-5} \text{ cm/s}. \quad (3)$$

A comparative analysis of the results of these two numerical experiments shows that with a decrease in the neutron flux density of the external source from $10^{23} \text{ cm}^{-2}\text{s}^{-1}$ to $10^{15} \text{ cm}^{-2}\text{s}^{-1}$, all other constants unchanged (the only difference is the time step of 5min in the latter case), the wave burning speed approximately doubled, and the wave half-width also increased significantly (evaluation was carried out using ^{239}Pu) from 10 cm to 100 cm.

An explanation of the change in the parameters of the burning regime, such as the phase velocity and the width of the wave burning zone, when only the flux density of the external source is changed, can be given if we recall the quantum-mechanical analogy for the diffusion equation for neutrons. The requirement to fulfill the Bohr-Sommerfeld quantization rule for solutions of this equation put forward by L.P. Feoktistov in [2], studied in [3], and later developed by V.D. Rusov *et al.* into the quantum-statistical Wigner distribution for phase velocities of the wave burning e.g. in [4, 5].

Indeed, in [4, 5] it allowed to write the critical condition for steady-state wave burning in the form:

$$I = \int \sqrt{\frac{n^{Pu239}}{n_{crit}^{Pu239}} - 1} dx = \frac{\pi}{2}, \quad (4)$$

where the integral is taken over the supercritical region $n^{Pu239} > n_{crit}^{Pu239}$.

As the simulation results show, even when only the flux density of the external source changes, within our simplified kinetic system, the width of the burning region changes, and according to (4), the ratio between n^{Pu239} and n_{crit}^{Pu239} must also change, since the integral should remain constant.

Hence we can make a conclusion about the change in the equilibrium-stationary and critical concentrations of ^{239}Pu which are the parameters in the Wigner quantum-statistical distribution for phase velocities of the wave burning [4, 5], and this causes the change in the wave burning speed.

Note that the presented simulation results clearly demonstrate the influence of the parameters of an external neutron source on the parameters of the burning regime even for the simplified model under consideration. In a real process of nuclear burning, not only the flux density of an external neutron source, but also its energy spectrum will have a significant effect on the burning regime.

According to the theory of a soliton-like neutron wave of slow nuclear burning, developed on the basis of the quantum chaos theory [4, 5], the neutron-nuclear burning speeds must satisfy the Wigner quantum-statistical distribution. The phase velocity u of a soliton-like neutron wave of nuclear burning is determined by the following approximate equality:

$$\Lambda(a_*) = \frac{u\tau_\beta}{2L} \cong \left(\frac{8}{3\sqrt{\pi}} \right)^6 a_*^4 \exp\left(-\frac{64}{9\pi} a_*^2\right), \quad a_*^2 = \frac{\pi^2}{4} \cdot \frac{N_{crit}^{Pu}}{N_{eq}^{Pu} - N_{crit}^{Pu}}, \quad (5)$$

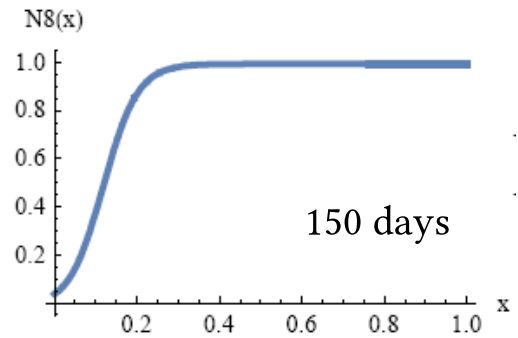
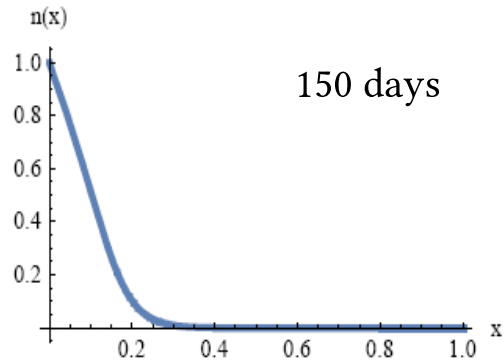
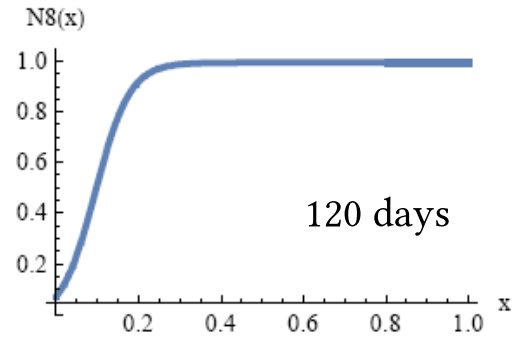
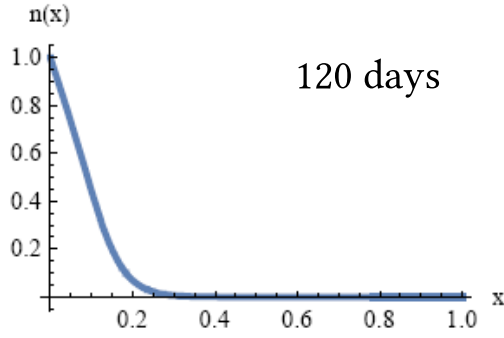
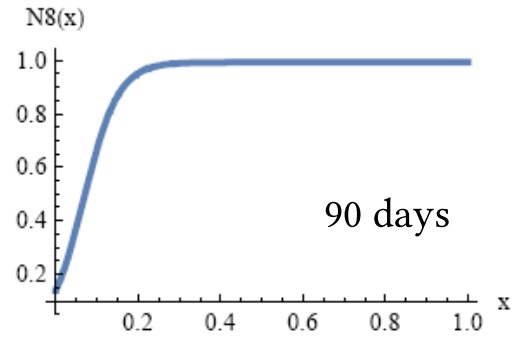
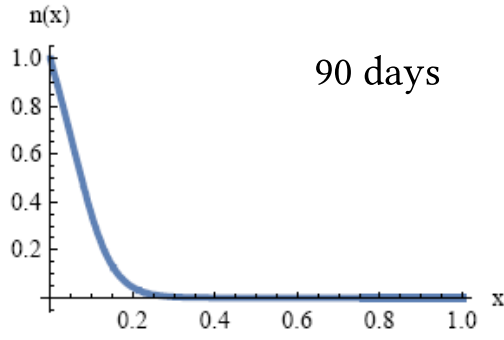
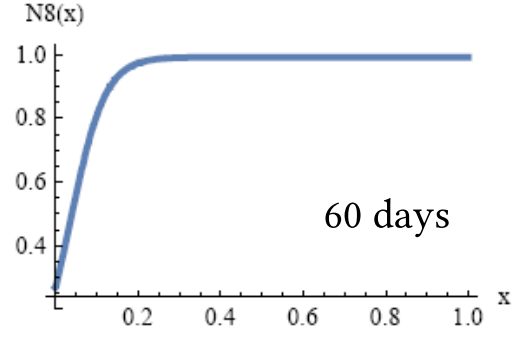
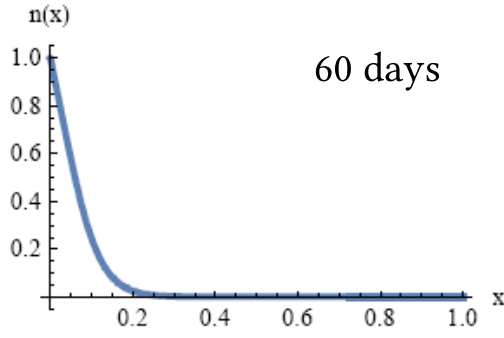
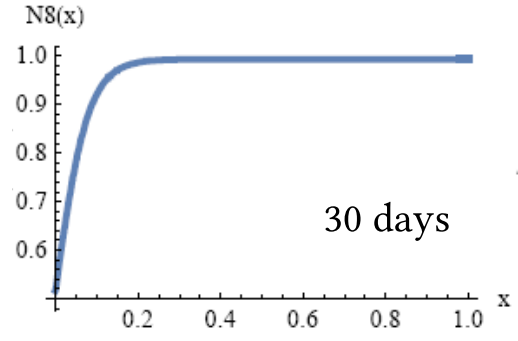
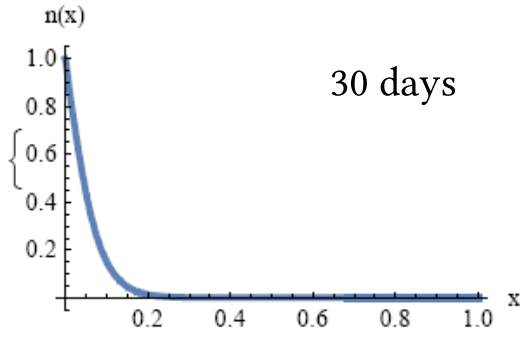


Figure 6: Kinetics of the neutrons density during the wave nuclear burning in natural uranium for the external neutron flux of $10^{15} \text{ cm}^{-2} \text{ s}^{-1}$. The dimensionless neutron density is plotted.

Figure 7: Kinetics of the ^{238}U density during the wave nuclear burning in natural uranium for the external neutron flux of $10^{15} \text{ cm}^{-2} \text{ s}^{-1}$. The dimensionless ^{238}U density is plotted.

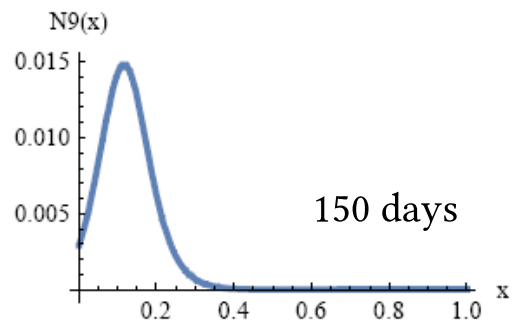
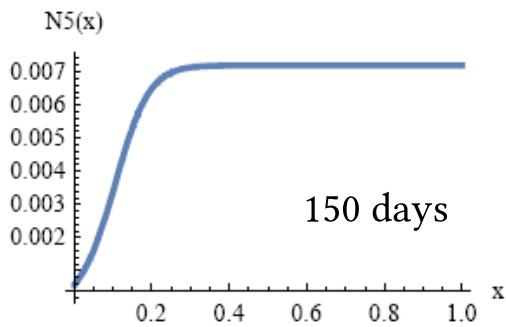
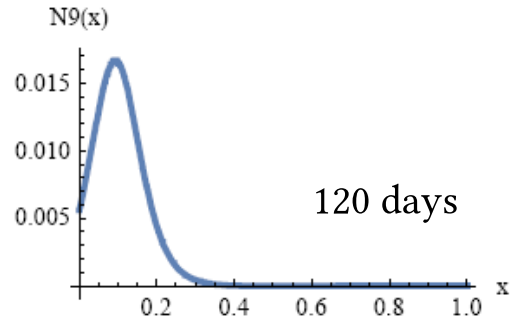
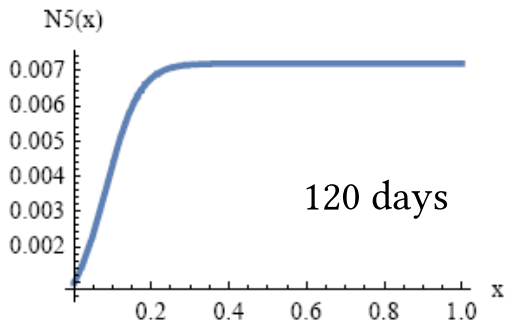
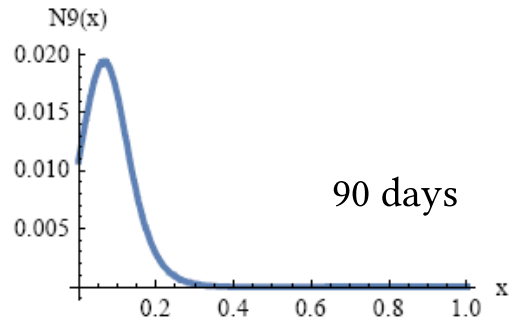
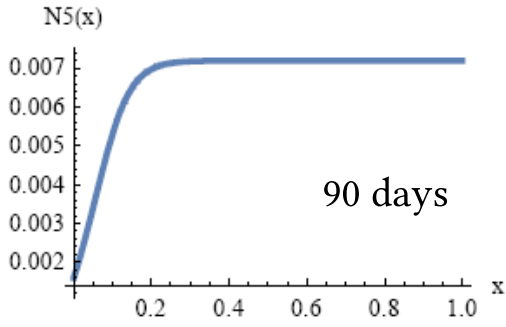
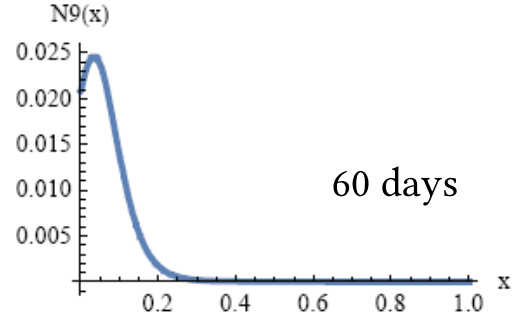
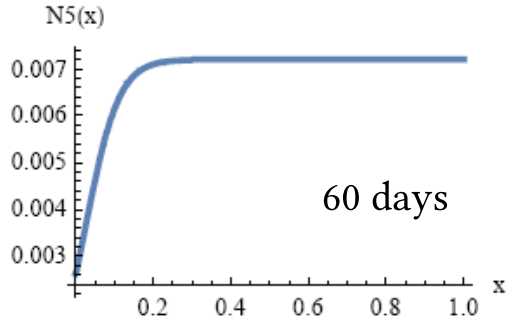
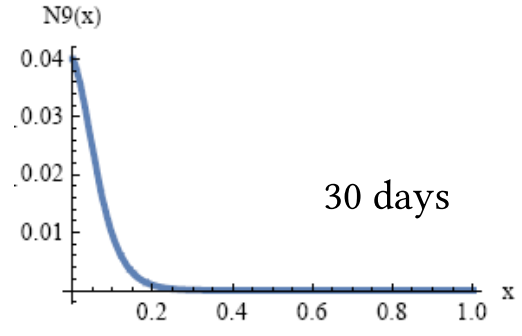
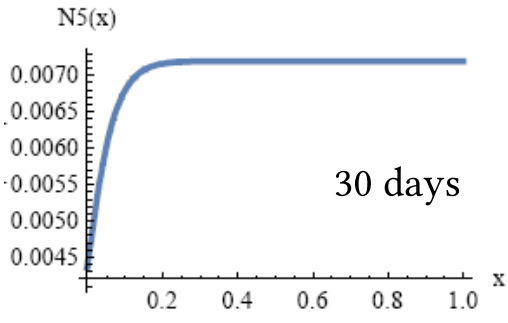


Figure 8: Kinetics of the ^{235}U density during the wave nuclear burning in natural uranium for the external neutron flux of $10^{15} \text{ cm}^{-2} \text{ s}^{-1}$. The dimensionless ^{235}U density is plotted.

Figure 9: Kinetics of the ^{239}U density during the wave nuclear burning in natural uranium for the external neutron flux of $10^{15} \text{ cm}^{-2} \text{ s}^{-1}$. The dimensionless ^{239}U density is plotted.

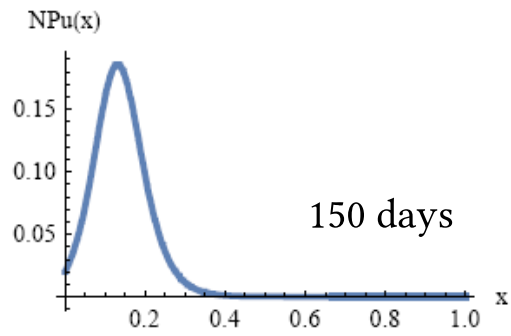
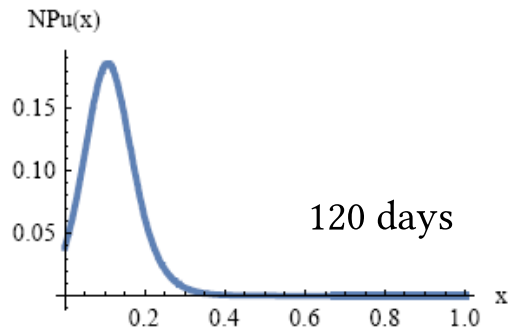
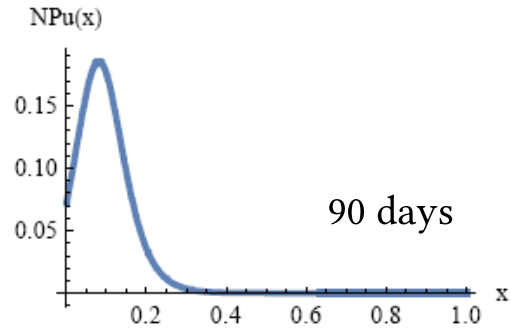
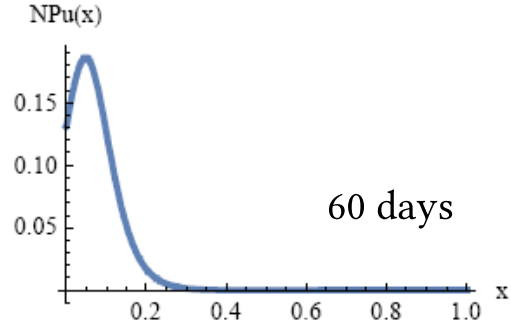
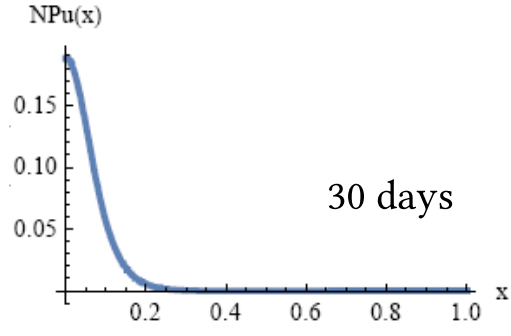


Figure 10: Kinetics of the ^{239}Pu density during the wave nuclear burning in natural uranium for the external neutron flux of $10^{15} \text{ cm}^{-2} \text{ s}^{-1}$. The dimensionless ^{239}Pu density is plotted.

where $\Lambda(a_*)$ is a dimensionless invariant, depending on the parameter a_* ; N_{eq}^{Pu} and N_{crit}^{Pu} are the equilibrium and critical concentrations of ^{239}Pu , L is the mean free path of neutrons, τ_β is the delay time, associated with the production of the active (fissile) isotope and equal to the effective period of the β -decay of compound nuclei in the Feoktistov uranium-plutonium cycle.

To check the correspondence between the Wigner distribution (5) and the phase velocity of the slow neutron-nuclear burning of natural uranium in the epithermal region of neutron energies, which is obtained by numerical simulation, let us make the corresponding estimates of the parameter a_*^2 and invariant $\Lambda(a_*)$.

For this we can use the data of numerical simulation at an external source flux density of $10^{15} \text{ cm}^{-2}\text{s}^{-1}$, shown in Fig. 10 for ^{239}Pu .

From fig. 10, one can find $N_{eq}^{Pu} \approx 0.19 \times 4.8 \cdot 10^{22} \text{ cm}^{-3}$ (maximum on the ^{239}Pu concentration curve) and $N_{crit}^{Pu} \approx 0.1 \times 4.8 \cdot 10^{22} \text{ cm}^{-3}$ (inflection point on the ^{239}Pu concentration curve).

Then, according to (5), for the parameter a_* and invariant $\Lambda(a_*)$ we obtain the following estimates:

$$a_* = \sqrt{\frac{\pi^2}{4} \frac{0.1 \cdot 10^{22} \text{ cm}^{-3}}{0.19 \cdot 10^{22} \text{ cm}^{-3}} \text{ cm}^{-3} - 0.1 \cdot 10^{22} \text{ cm}^{-3}} = \sqrt{\frac{\pi^2}{4} \frac{0.1}{0.09}} \approx 1.66 \quad \text{and} \quad \Lambda(a_*) \approx 0.3. \quad (6)$$

These estimates for a_* and $\Lambda(a_*)$ are shown in Fig. 11.

In order to estimate the phase velocity of the wave burning from these parameters, we first have to estimate the mean free path for epithermal neutrons in the studied medium.

The mean free path for neutrons of the indicated epithermal region of neutron energies is:

$$L = \frac{1}{\Sigma_a} = \frac{1}{\bar{\sigma}_c^9 N_8(t=0)} \approx \frac{1}{4.68 \cdot 10^{-24} \text{ cm}^2 \cdot 0.48 \cdot 10^{23} \text{ cm}^{-3}} \approx 4.45 \text{ cm}. \quad (7)$$

Then from expression (5) we can also obtain an estimate for the phase velocity of burning:

$$u = \frac{2 \cdot \Lambda \cdot L}{\tau_\beta} \approx \frac{2 \cdot 0.3 \cdot 4.45 \text{ cm}}{2.85 \cdot 10^5 \text{ s}} \approx 0.94 \cdot 10^{-5} \text{ cm/s}. \quad (8)$$

A comparison of (3) and (8) demonstrates a rather good agreement.

It is also possible to estimate the heat power produced by the reactor with the active zone of natural uranium, provided the wave burning mode is realized in it.

Indeed, given that the derivative of the ^{239}Pu concentration with respect to time and the derivative with respect to the coordinate are related by the following equation:

$$\frac{dN^{Pu239}}{dt} = u \frac{dN^{Pu239}}{dx}, \quad (9)$$

where u is the wave burning speed for the case of external source with neutron flux density of $10^{15} \text{ cm}^{-2}\text{s}^{-1}$, according to Fig. 10, it is possible to calculate the specific heat power P_{spec} :

$$\begin{aligned} P_{spec} &\approx 210.3 \text{ MeV} \cdot \frac{dN^{Pu239}}{dt} = 210.3 \text{ MeV} \cdot u \frac{dN^{Pu239}}{dx} \approx \\ &\approx 210.3 \text{ MeV} \cdot 0.77 \times 10^{-5} \times 0.48 \cdot 10^{22} \frac{1}{\text{cm}^3 \cdot \text{s}} \approx 77.73 \cdot 10^{17} \frac{\text{MeV}}{\text{cm}^3 \cdot \text{s}} \approx \\ &\approx 77.73 \cdot 10^{23} \times 1.6 \cdot 10^{-19} \frac{\text{J}}{\text{cm}^3} \approx 1.24 \frac{\text{MW}}{\text{cm}^3}. \end{aligned} \quad (10)$$

For an example active zone in a form of a cylinder with 50cm diameter, the estimate of the burning zone volume is:

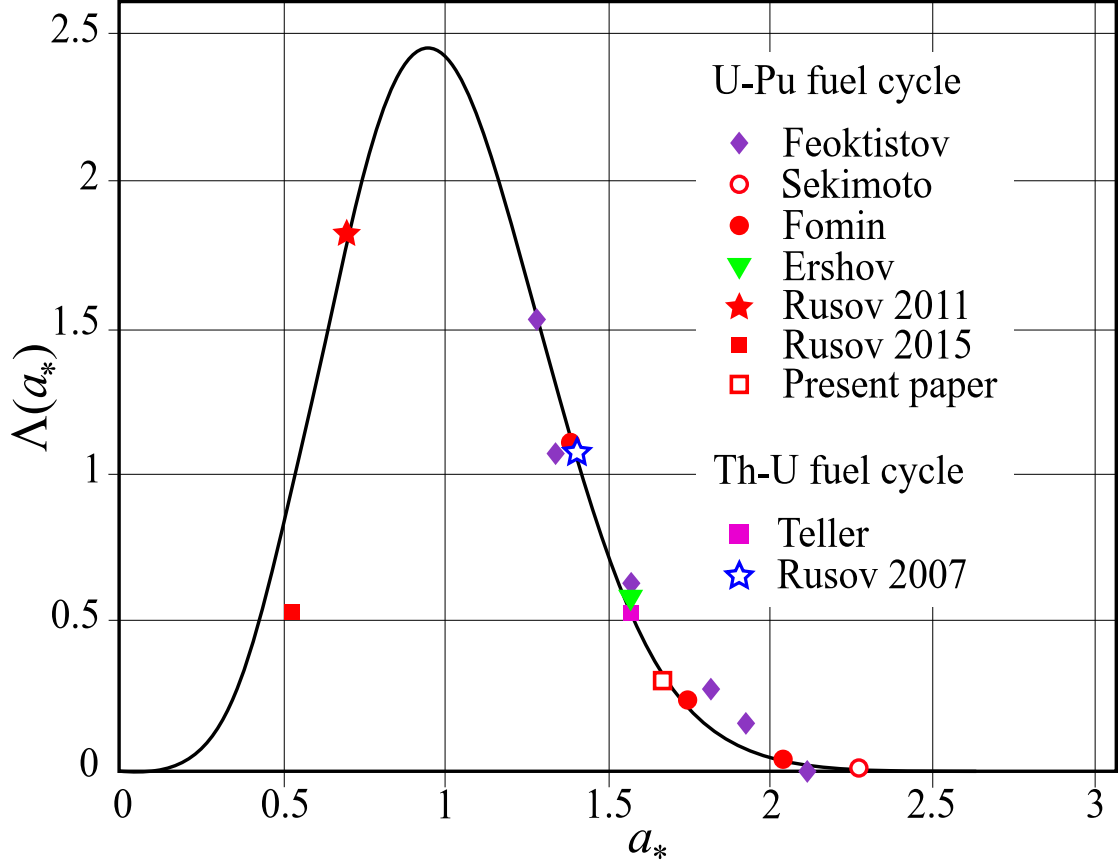


Figure 11: Theoretical (solid line) and calculated (points) dependence for the phase velocity of neutron-nuclear burning $\Lambda(a_*) = u\tau_\beta/2L$ on the parameter a_* . Data combined from [1, 4–13], and supplemented by the estimate obtained in the present paper for slow wave burning of natural uranium in the epithermal region of neutron energies (1.0 - 7.0 eV).

$$V_{burning} \approx \pi \cdot r^2 \cdot L \approx 3.14 \cdot (25 \text{ cm})^2 \cdot 4.45 \text{ cm} \approx 8730 \text{ cm}^3 \quad (11)$$

And the resulting heat power is:

$$P = P_{spec} \cdot V_{burning} \approx 1.24 \frac{\text{MW}}{\text{cm}^3} 8730 \text{ cm}^3 \approx 10.8 \text{ GW}. \quad (12)$$

It should be noted that the simulated kinetics of neutron density presented in Figs. 1 and 6, does not demonstrate the neutron wave, in contrast to the previously published results for the ^{238}U wave burning in fast neutron range (neutron energy $\sim 1 \text{ MeV}$) [4, 5].

We believe that this is related to the use of a permanent external source of neutrons, as in [1], with a rather high flux density, which hides the neutron wave on its background.

3. Conclusions

We presented new results of two computer simulations of the epithermal neutron-nuclear burning in natural uranium for two different densities of the external neutron flux. Each simulation represents about half a year of reactor operation.

The obtained results clearly demonstrate the influence of the external neutron source parameters on the burning mode even for the simplified model under consideration.

In a real process of nuclear burning, not only the flux density of an external neutron source, but also its energy spectrum will have a significant effect on the burning regime.

Based on the simulation results, we estimate the wave burning speed and the corresponding heat power production of the epithermal wave nuclear reactor with a homogeneous cylindrical core with a diameter of 50 cm made of natural uranium and a moderator. The resulting power of such reactor is about 10 GW.

Acknowledgements

M.V. Eingorn acknowledges support by NSF CREST award HRD-0833184 and NASA grant NNX09AV07A and thanks Prof. Branislav Vlahovic (NCCU) for the given computational resources without which the numerical calculation would be impossible on the same level of accuracy.

References

- [1] V. Rusov, V. Tarasov, M. Eingorn, S. Chernezhenko, A. Kakaev, V. Vashchenko, M. Beglaryan, Ultraslow wave nuclear burning of uranium–plutonium fissile medium on epithermal neutrons, *Progress in Nuclear Energy* 83 (2015) 105 – 122. doi:<https://doi.org/10.1016/j.pnucene.2015.03.007>.
- [2] L. Feoktistov, Neutron-fission wave, *Dokl. Akad. Nauk SSSR* (309) (1989) 4–7.
- [3] A. P. Ershov, V. F. Anisichkin, Natural neutron-fission wave, *Combustion, Explosion and Shock Waves* 39 (2) (2003) 226–231. doi:[10.1023/A:1022925403499](https://doi.org/10.1023/A:1022925403499).
- [4] V. D. Rusov, E. P. Linnik, V. A. Tarasov, T. N. Zelentsova, I. V. Sharph, V. N. Vaschenko, S. I. Kosenko, M. E. Beglaryan, S. A. Chernezhenko, P. A. Molchinikolov, S. I. Saulenko, O. A. Byegunova, Traveling wave reactor and condition of existence of nuclear burning soliton-like wave in neutron-multiplying media, *Energies* 4 (9) (2011) 1337–1361. doi:[10.3390/en4091337](https://doi.org/10.3390/en4091337).
- [5] V. D. Rusov, V. A. Tarasov, I. V. Sharph, V. N. Vashchenko, E. P. Linnik, T. N. Zelentsova, M. E. Beglaryan, S. A. Chernegenko, S. I. Kosenko, V. P. Smolyar, On some fundamental peculiarities of the traveling wave reactor, *Science and Technology of Nuclear Installations* 2015 (2015) 1–23. doi:[10.1155/2015/703069](https://doi.org/10.1155/2015/703069).
- [6] E. Teller, M. Ishikawa, L. Wood, Completely automated nuclear reactors for long-term operation, in: *Conference: Joint American Physical Society and the America Association of Physics Teachers Texas meeting*, 26-28 Oct 1995, Lubbock, TX (United States), 1995.
- [7] E. Teller, M. Ishikawa, L. Wood, R. Hyde, J. Nuckolls, Completely automated nuclear reactors for long-term operation ii: Toward a concept-level point-design of a high-temperature, gas-cooled central power station system, part ii, in: *Proceedings of the International Conference on Emerging Nuclear Energy Systems, ICENES’96*, Obninsk, Russian Federation, Obninsk, Russian Federation, Obninsk, Russian Federation, 1996, pp. 123–127, also available from Lawrence Livermore National Laboratory, California, publication UCRL-JC-122708-RT2.
- [8] V. Rusov, V. Pavlovich, V. Vaschenko, V. Tarasov, T. Zelentsova, V. Bolshakov, D. Litvinov, S. Kosenko, O. Byegunova, Geoantineutrino spectrum and slow nuclear burning on the boundary of the liquid and solid phases of the earth’s core, *J. Geophys. Res.* 112, b09203 (2007). doi:[10.1029/2005JB004212](https://doi.org/10.1029/2005JB004212).

- [9] H. Sekimoto, Y. Udagawa, Effects of fuel and coolant temperatures and neutron fluence on candle burnup calculation, *Journal of Nuclear Science and Technology* 43 (2) (2006) 189–197. [doi:10.1080/18811248.2006.9711081](https://doi.org/10.1080/18811248.2006.9711081).
- [10] S. Fomin, Y. Mel'nik, V. Pilipenko, N. Shul'ga, Investigation of self-organization of the non-linear nuclear burning regime in fast neutron reactors, *Annals of Nuclear Energy* 32 (13) (2005) 1435–1456. [doi:10.1016/j.anucene.2005.04.001](https://doi.org/10.1016/j.anucene.2005.04.001).
- [11] S. Fomin, Y. Mel'nik, V. Pilipenko, N. Shulga, Self-sustained regime of nuclear burning wave in U-Pu fast reactor with Pb-Bi coolant, *Problems of Atomic Science and Technology* 3 (2007) 156–163.
- [12] V. D. Rusov, E. P. Linnik, V. A. Tarasov, T. N. Zelentsova, I. V. Sharf, S. A. Chernezhenko, O. A. Byegunova, “Quantum” chaos and stability condition of soliton-like waves of nuclear burning in neutron-multiplicating media, in: *CHAOS 2011 - 4th Chaotic Modeling and Simulation International Conference, Proceedings*, 2019, pp. 509–534.
- [13] V. N. Pavlovich, E. N. Khotyaintseva, V. D. Rusov, V. N. Khotyaintsev, A. S. Yurchenko, Reactor operating on a slow wave of nuclear fission, *Atomic Energy* 102 (3) (2007) 181–189. [doi:10.1007/s10512-007-0027-x](https://doi.org/10.1007/s10512-007-0027-x).